EUROPEAN RESPIRATORY journal

FLAGSHIP SCIENTIFIC JOURNAL OF ERS

Early View

Original article

Cathepsin B promotes collagen biosynthesis driving Bronchiolitis Obliterans Syndrome

Carmela Morrone, Natalia F. Smirnova, Aicha Jeridi, Nikolaus Kneidinger, Christine Hollauer, Jonas Christian Schupp, Naftali Kaminski, Dieter Jenne, Oliver Eickelberg, Ali Önder Yildirim

Please cite this article as: Morrone C, Smirnova NF, Jeridi A, *et al*. Cathepsin B promotes collagen biosynthesis driving Bronchiolitis Obliterans Syndrome. *Eur Respir J* 2020; in press (https://doi.org/10.1183/13993003.01416-2020).

This manuscript has recently been accepted for publication in the *European Respiratory Journal*. It is published here in its accepted form prior to copyediting and typesetting by our production team. After these production processes are complete and the authors have approved the resulting proofs, the article will move to the latest issue of the ERJ online.

Copyright ©ERS 2020

Title page

Cathepsin B promotes collagen biosynthesis driving Bronchiolitis Obliterans Syndrome

Carmela Morrone[1], Natalia F. Smirnova[2], Aicha Jeridi[1], Nikolaus Kneidinger[3, 4], Christine Hollauer[1], Jonas Christian Schupp[5], Naftali Kaminski[5], Dieter Jenne[1, 6], Oliver Eickelberg[2,7], and Ali Önder Yildirim[1].

[1]Comprehensive Pneumology Center, Institute of Lung Biology and Disease, Helmholtz Zentrum München; Member of the German Center for Lung Research (DZL); [2]Division of Pulmonary Sciences and Critical Care Medicine, University of Colorado, Anschutz Medical Campus, Aurora, CO, USA; [3]Department of Internal Medicine V, Ludwig-Maximilians-University (LMU) of Munich, Germany; [4]Comprehensive Pneumology Center (CPC-M), Member of the German Center for Lung Research (DZL), Munich, Germany; [5]Pulmonary, Critical Care and Sleep Medicine, Yale School of Medicine, New Haven, CT, USA; [6]Max Planck Institute of Neurobiology, Planegg-Martinsried 82152, Germany [7]Division of Pulmonary, Allergy, and Critical Care Medicine, Department of Medicine, University of Pittsburgh, PA, USA

Take home message: CatB as a new biomarker and therapeutic target for early bronchiolitis obliterans syndrome (BOS) after lung transplantation

Authors contributions: C.M, N.F.S., O.E., A.O.Y. designed experiments; C.M. performed all the experiments and analysed data; A.J. provided feedback in Figure 5; N.F.S., A.O.Y oversaw all data analysis; N.K. provided human BAL fluid and clinical information; CH performed tissue staining; JCS and NKa performed single-cell re-analysis; N.F.S. performed the LTx murine surgeries; C.M drafted the manuscript; C.M, A.J., N.F.S. and A.O.Y corrected the manuscript. All authors have critically revised the manuscript. All authors have read, reviewed, and approved the final manuscript as submitted to take public responsibility for it.

Correspondence and requests for reprinting should be addressed to **Ali Önder Yildirim**, Director & Head of Research Group, Institute of Lung Biology and Disease (ILBD), Comprehensive Pneumology Center (CPC), Helmholtz Zentrum Muenchen, Munich, Germany. Phone: 0049-89-3187-4037; Fax: 0049-89-5160-2400; E-mail: oender.yildirim@helmholtz-muenche.de; and **Oliver Eickelberg**, Professor of Medicine, Division of Pulmonary, Allergy, and Critical Care Medicine, Vice Chair for Basic and Translational Sciences, Department of Medicine-University of Pittsburgh, Pittsburgh, PA 15261; E-mail: oliver.eickelberg@pitt.edu

Abstract

Bronchiolitis obliterans syndrome (BOS) is a major complication after lung transplantation (LTx). BOS is characterized by massive peribronchial fibrosis, leading to air trapping induced pulmonary dysfunction. Cathepsin B, a lysosomal cysteine-protease, was shown to enforce fibrotic pathways in several diseases. However, the relevance of Cathepsin B in BOS progression has not yet been addressed. The aim of the study was to elucidate the function of Cathepsin B in BOS pathogenesis.

We determined Cathepsin B levels in BAL fluid and lung tissue from healthy donors (HD) and BOS LTx patients. Furthermore, Cathepsin B activity was assessed via a FRET-based assay and protein expression was determined using Western blotting, ELISA, and immunostaining. To investigate the impact of Cathepsin B in the pathophysiology of BOS, we used an *in-vivo* orthotopic left-LTx mouse model. Mechanistic studies were performed *in-vitro* using macrophage and fibroblast cell lines.

We found a significant increase of Cathepsin B activity in BALF and lung tissue from BOS patients, as well as in our murine model of lymphocytic bronchiolitis (LB). Moreover, Cathepsin B activity was associated with an increased biosynthesis of collagen, and negatively affected lung function. Interestingly, we observed that Cathepsin B was mainly expressed in macrophages that infiltrated areas characterized by a massive accumulation of collagen deposition. Mechanistically, macrophage-derived Cathepsin B contributed to TGF-β1-dependent activation of fibroblasts, and its inhibition reversed the phenotype.

Infiltrating macrophages release active Cathepsin B promoting fibroblast-activation and subsequent collagen deposition, driving BOS. Cathepsin B represents a promising therapeutic target to prevent the progression of BOS.

Keywords: lung transplantation; bronchiolitis obliterans syndrome; fibrosis; macrophages: fibroblasts; Cathepsin B, collagen

Introduction

Patients with severe end-stage lung disease rely on lung transplantation (LTx) as the only promising therapeutic intervention [1]. Long-term outcomes are affected by high incidence of bronchiolitis obliterans syndrome (BOS) [2, 3]. Histological evidences have defined BOS with a severe mononuclear infiltration of airways [4], vessels and septum [5], associated with fibrosis [6], that contribute to a decline in FEV_1 [7]. However, the main triggers for BOS development have not yet been identified. Epithelial-mesenchymal transition (EMT) plays a key-role in the fibro-proliferative process [8], deriving from the self-perpetuating activation of fibroblasts, and massive release of collagen. Collagen deposition results in peri-bronchiolar fibrosis and declined in pulmonary functions [9]. Transforming growth factor-beta-1 (TGF-β1) is a well-described pro-fibrotic factor, which is released in the extracellular space bound to a latency-associated protein (LAP) that prevents its immediate activation [10]. Dissociation and activation depend on different triggers [11]. Active TGF-β1 binds to its receptor, and downstream signaling results in the regulation of pro-fibrotic genes, including collagen. Cathepsin B (CatB), a cysteine-protease, whose activity is negatively regulated by Cystatin-C (CysC) [12] was shown to implement TGF-β1 signaling [13], and significantly increased in bleomycin-induced lung fibrosis [14] and in liver fibrosis [15]. Lung tissue from BOS patients revealed increased levels of TGF-β1 [16]. In this study, we investigated targets that are crucial in the pathogenesis of BOS. We found a direct association between CatB activity and the increase of pro-collagen-1a1 in human BOS as well as in mouse LB samples. Prevention of BOS development after LTx in mice lacking CatB illustrates the importance of our findings. Interestingly, infiltrating pro-inflammatory macrophages were the major source of CatB that mechanistically contributed to the TGF-β1-dependent activation of fibroblasts. In summary, our study is the first that shows CatB as promoter of BOS progression, and mechanistically interrogates

the role of CatB in its pathogenesis. This data supports the consideration of CatB inhibitors as a potential therapy for the treatment of BOS in LTx patients.

Methods

See online supplement for additional details.

Human Subjects

Human studies were approved by the local ethics committees. Two cohorts of LTx patients were studied. Frozen human BALF samples and lung tissue from Munich-cohort (Ludwig-Maximilian University, protocol 333-10), and BOS stage-3 lung tissue from France-cohort (protocol N8CO-08-003, ID RCB 2008-A00485-50).

BALF samples were retrospectively collected from our bioarchive, where they were stored longitudinally. In total 20 consecutive stable LTx patients, who did not develop CLAD until the preparation of the manuscript (and at least after 5 years from BAL collection), and 22 consecutive BOS patients were considered. BALF samples analyzed for the BOS-0, BOS-1, BOS-2, and BOS-3 group correspond to the same 22 BOS patients with serial samples along with post-Tx time and disease-stage (for a total number of n=20 for BOS-0, n=13 for BOS-1, n=13 for BOS-2 and n=20 for BOS-3).

BOS stages and relative BALF samples were grouped according to the % decline in FEV_1 values of baseline: they were grouped in BOS-0 patients if they were stable at the time of BAL collection, but developed later BOS-1 or higher; in BOS-1 when the FEV_1 value was between 66-80%; in BOS-2 when the FEV_1 value was between 51-65%; and in BOS-3 when the FEV_1 value was ≤50% [1, 2]. Stable LTx patients did not develop CLAD for at least 5 years from the time the BAL sample was collected. Patients with infection as cause for lung function decline were not included in the study. Acute cellular rejection>A1 was not present in any of the BOS samples at the time of BAL collection.

We selected patients solely according to lung function analysis and not on differential BAL cell count. Stable LTx patients with high percentage (%) number of BALF neutrophils, and low % number of BALF macrophages, were completely asymptomatic, and remained stable over a long period of time (> 5 years) from the BAL collection.

BALF samples were collected from patients affected by lung fibrosis (LF) which includes idiopathic pulmonary fibrosis (IPF) and non-IPF patients; patients affected by chronic obstructive pulmonary disease (COPD), cystic fibrosis (CF) and pulmonary hypertension (PH). A more detailed description of the clinical assessment in LTx patients was previously described by Kneidinger et al. [17].

Human lung tissue

Paraffin-embedded lung tissue sections were obtained from two sources. The control group used in this study was provided by our BioArchive (CPC, Munich) and derived from healthy parts of lungs from non-transplanted donors, that we called “Healthy donors, HD” lung tissue. The “BOS” lung tissue was provided by the Hospital Marie-Lannelongue, Le Plessis-Robinson, France, and derived from BOS-stage 3 lung tissue. Detailed information is provided in the **Supplemental Figure 1f.**

Procollagen1a1 levels in frozen human BALF: Procollagen1a1 levels were measured via an enzyme-linked immunosorbent assay

Cathepsin B activity and protein levels in BALF, cell medium, and in paraffin-embedded lung tissue: Cathepsin B activity was measured via a FRET-probe based activity assay. Cathepsin B protein-level in BALF were measured using Western blotting. Cathepsin B tissue expression was measured using immunohistochemistry and immunofluorescence stainings.

Animal experiments

Animal experiments were approved by the local government of upper Bavaria, Germany (project 55.2-1-54-2532.120.2015). Male C57BL/6, HLA *(C57BL/6-Tg (HLA-A2.1)1Enge/J*) were used as donor of left lobes, and *Ctsb*$^{-/-}$ (*B6;129-Ctsbtm1Jde/J*) and C57BL/6 as recipient mice.

Orthotopic left lung mouse transplantation: The surgery was performed as previously described [18] .

Left-lung function: Mice were anesthetized with a mixture of medetomidine (1 mg/kg), midazolam (0.05 mg/kg), and fentanyl (0.02 mg/kg), then intubated and connected to a Minivent-ventilation system (120 breaths/min, volume of 300µl). The chest was opened, and the right bronchus was clamped. Then, mice left lung function was measured via FlexiVent system (Scireq) (tidal volume of 3.5 ml/kg, frequency of 150 breaths/min). Airway compliance, resistance, tissue elastance and inspiratory capacity were measured via SnapShot, Prime-8 and Quick-prime wave perturbations. Three readings per animal were taken.

BAL collection: BAL collection was performed as previously described [18]. BAL was centrifuged and BAL supernatant, BAL fluid (BALF) was stored at -80°C for further analysis. In this study we used all the 83 available BALF (1 ml) samples that were collected from 20 Stable LTx patients, as well as 22 BOS patients at different stages of the disease (providing BALF samples of n=20 for BOS-0, n=13 for BOS-1, n=13 for BOS-2 and n=20 for BOS-3).

Tissue inflammation and collagen: Inflammation and collagen were analyzed via Masson´s trichrome staining (see online supplement) and CAST analysis.

Gal3+ and CatB+ cells quantification was performed by considering 20 random images (20x objective) (FOV), and then counting the actual number of cells detectable. Values were normalized to the total area.

CAST: A computer assisted stereological toolbox (newCAST, Visiopharm) and an Olympus BX51-light microscope were used for the quantification of inflammation and collagen. The software selects 35 random fields of view across multiple lung sections using the 40x objective. The area of collagen deposition or inflammation is then calculated in each FOV, determined by the number of points hitting the area ($P_{collagen}$). In addition, however, intercepts of lines with the basement membrane of airways and blood vessels is then recorded ($I_{airway+vessel}$), meaning the volume of collagen or inflammation is normalized to the surface area of the basal membrane across the lung using the formula $V/S = \sum P_{collagen} \times L(p) / \sum_{Iairway+vessel}$, where L(p) is the line length per point. This normalization to basement membrane surface area prevents over or underestimation of the results".

Immunohistochemistry staining of human and mouse lung tissue: see online supplement

***In vitro* experiments:** A macrophage and a fibroblast cell-line were used for simulating the mechanism of chronic rejection *in-vitro*. See online supplement.

Statistics: Data represent mean ± SEM. For the comparison between 2 groups, the statistical significance was evaluated by a non-parametric t-test (Mann-Whitney); for the comparison between more than 2 groups (except those including BOS grades), the statistical significance was evaluated by one-way ANOVA followed by a Kruskal-Wallis post-test or followed by a Tukey's multiple -test. Furthermore, for the comparison between Stable LTx patients and BOS grades, the stable group was compared to each BOS group via a non-parametric t-test (Mann-Whitney), because Stable LTx patient group is independent from BOS group. The values at the different BOS grades (not independent of each other) were compared with the others, with a Mixed effects model analysis followed by a Tukey's multiple comparisons test, which takes into account the fact that not all samples for each patients have been collected at each time-point. Median values are showed. Differences were considered to be statistically significant at $P < 0.05$.

Results

Cathepsin B levels are increased in human BOS

Patients with BOS are characterized by marked tissue-collagen deposition that negatively affects long-term functional outcomes [19, 20]. Pro-collagen-1a1 is a well-described marker of fibroblast activation [21-23]. Therefore, we measured soluble pro-collagen-1a1 levels in bronchoalveolar lavage fluid (BALF) using an enzyme-linked immunosorbent assay (ELISA).

BALF samples were retrospectively collected from our bioarchive, and a total number of 20 Stable LTx patients and 22 BOS patients were analyzed. When comparing the median value of BALF samples from Stable LTx patients (S), who did not develop signs of chronic lung allograft dysfunction during the entire study, with the median value of BALF at each stage of the disease in BOS patients (BOS 0-3), who showed a significant decline of FEV_1%, but no a persistent change in total lung capacity (TLC %) and in BALF total protein amount (**Suppl. Fig 1a-e,** Munich cohort), we found a large increase of newly formed pro-collagen-1a1 in BALF from BOS patients (7.4 fold change, P= 0.0003) (**Figure 1a**). Pro-collagen-1a1 levels were already high at stage-1 of the disease (655.02 pg/ml in BOS-1 vs 98.8 pg/ml in S, P= 0.0009), and stage-2 of the disease (425.31 pg/ml in BOS-2 vs 98.8 pg/ml in S, P=0.029), and peaked at stage-3 (1081.74 pg/ml in BOS-3 vs 98.8 in S, P= 0.0048) (**Figure 1b**) when compared with stable LTx patients. No significant differences were found between the BOS groups after using a Mixed effects model analysis followed by a Tukey's multiple comparisons test. Furthermore, pro-collagen-1a1 levels negatively correlated with FEV_1 % after LTx (P= 0.0018) (**Figure 1c**). These results suggest specific up-regulation of fibroblast activation in lungs of patients along the progression of BOS. Because CysC, an endogenous regulator of the activity of CatB, was shown to prevent excessive proliferation and activation of fibroblasts in injured lungs [24] and in cancer cells [25] we determined CysC levels in explanted human lungs via immunostaining. In comparison to healthy donors (HD), lung tissue from BOS stage-3 patients

(**Suppl. Fig 1f,** France Cohort) showed a remarkable decrease in CysC expression (35.3 positive cells/20 FOV in S, vs 14.3 positive cells/20 FOV in BOS-3, P= 0,011) (**Suppl. Fig 2a-b**) in macrophages (**Suppl. Fig 2c**). CatB was already reported to be notably increased in lung fibrosis [14], and in liver fibrosis [15]. We therefore hypothesized that the activity of CatB in BALF from BOS patients is dysregulated as a consequence of decreased levels of CysC. We indeed observed a substantial increase of CatB activity in BOS patients (16.62ng/ml in BOS vs 2.69 ng/ml in S, P= 0.0001) (**Figure 1d**), starting already at early stage of deterioration in allograft function (BOS-0) (16.9 ng/ml in BOS-0 vs 2.69 ng/ml in S, P<0.0001) compared to Stable LTx patients (**Figure 1e**). No significant differences were found between the BOS groups after using a mixed effects model analysis followed by a Tukey's multiple comparisons test. Remarkably, CatB expression was also significantly increased in BALF and in lung tissue of BOS patients (**Figure 1h-k**).

Moreover, CatB activity negatively correlated with FEV_1 % values from baselines after LTx, similarly to pro-collagen-1a1 levels (P= 0.014) (**Figure 1f**). Interestingly, a more in-depth investigation of CatB activity revealed a substantial increase in patients previously diagnosed for lung fibrosis (LF) (53.9 ng/ml in BOS vs 7.3 ng/ml in, P= 0.0047) (**Suppl. Fig 2d**), but not for other lung diseases (**Suppl. Fig 2e**). Notably, BOS patients diagnosed for LF showed decreased CysC levels in BALF samples compared with patients without signs of BOS (23.3 ng/ml in BOS vs 81.57 ng/ml in, P= 0.0048) (**Suppl. Fig 2f**). This increase was not observed in patients with "Other lung disease" (51.7 ng/ml in BOS vs 68.3 ng/ml in S, P=0.6) (**Suppl. Fig 2g**). Moreover, CatB activity corresponded to the release of pro-collagen-1a1 in BALF from BOS patients, and correlated with disease progression (**Figure 1g**). Taken together, these results suggest that CatB activity is crucial for collagen expression and represents a key player in the progression of BOS. These findings were confirmed in two different cohorts of BOS patients (Munich and France cohort, **Suppl. Fig 1a, f**).

Infiltrating macrophages are the main source of Cathepsin B during BOS development

Since the influx of T, B cells, and macrophages has been observed in areas surrounding airways and vessels in the allografts, we investigated the expression of CatB in those cells. Using lung tissue from LTx patients as well as from our mouse model of LB that clearly shows pathological changes of human BOS [18], we identified enhanced macrophages number localizing to areas surrounding the airways and vessels as the main source of CatB (**Figure 2a**). Despite some neutrophils showed a weak CatB expression, T and B cells did not show any (**Suppl. Fig 4a-c**). Quantitative analysis of lung tissue from LB mice at 2 months revealed a large increase of infiltrating macrophages (324 macrophages/FOV in LB mice vs 97 macrophages/FOV in Ctrl mice; P= 0.0079) (**Figure 2b, c**), and of CatB-positive cells (110 CatB positive cells/FOV in LB mice, vs 5 CatB positive cells/FOV in Ctrl mice; P= 0.04) (**Figure 2d**) compared with control mice. Interestingly, only infiltrating macrophages that were negative for HLA.A2, expressed CatB, suggesting that recipient-derived macrophages are the main source of CatB in LB (**Figure 2e**). Strikingly, in accordance with our previous findings (**Suppl. Fig. 2c**), three different single-cell transcriptome analyses [26-28] of lung tissue, explanted from IPF patients at the time of LTx, showed an increase of CatB expression in macrophages (**Suppl. Fig.3a-b**), mainly in lung fibrosis (LF) patients. These findings strongly suggest that monocyte-derived macrophages are the main cell type expressing CatB in human and mouse lungs during the development of BOS.

Cathepsin B expression increases during the development of BOS in an orthotopic murine model of LB

To determine the contribution of CatB during disease progression, we analyzed the time-dependent expression of CatB in the orthotopic left LTx murine model. Left lungs from wildtype (B6) and HLA-A2–knock-in (HLA) mice were orthotopically transplanted into B6 mice and analyzed

at day 7, 14, and 28 after LTx (**Figure 3a**). We could demonstrate a time-dependent increase of inflammation and collagen deposition in areas surrounding airways, vessels and alveolar septum in the mismatched LTx mice reminiscent of human LB (**Figure 3b, c).** Consistent with human data (**Figure 1d, e**) we observed an increase of CatB expression in lung tissue and BALF of LB mice already after 14 days (**Figure 3d-f**). As we found human and here mouse CatB expression being positively associated with collagen deposition and disease progression, we analyzed the expression of ECM components critical for BOS progression. Collagen1a1 expression was increased in LB lung tissue after 14 days (**Figure 3e**). Fibronectin-1 (FN1), required for collagen matrix assembly and important in fibrosis [29], similar to CatB and collagen 1a, was also increased after 14 days in LB mice (**Figure 3e, f**). These results suggest a positive functional association between CatB expression and the biosynthesis of lung pro-fibrotic markers during BOS development.

Cathepsin B deficiency protects lung grafts from collagen deposition in LB

To elucidate whether CatB deficiency affects collagen deposition during the progression of LB, we investigated transplanted HLA.A2 lungs (Ctrl) into wild-type (B6) or *Ctsb*$^{-/-}$ mice and evaluated LB development after 28 days (**Figure 4a**). The control (Ctrl) is the left lung from non-transplanted HLA.A2 mice, for which the lung function has been measured after clamping the right bronchus, as for the transplanted mice. Strikingly, genetic deletion of CatB in recipient mice efficiently protected the allograft from LB progression. Allograft from CatB-deficient mice demonstrated improved lung compliance (0.017 ml/cmH_2O in *Ctsb*$^{-/-}$ mice, vs 0.0069 ml/cmH_2O in BOS mice; P= 0.011), and higher inspiratory lung capacity (0.31 ml in *Ctsb*$^{-/-}$ mice, vs 0.13 ml in BOS mice, P=0.017) in comparison to LB mice. Nevertheless, we observed no differences in the lung function between non-transplanted CatB-deficient and WT mice. Furthermore, *Ctsb*$^{-/-}$allografts were protected from a large increase in airway resistance (1.5 cmH_2O/ml in *Ctsb*$^{-/-}$ mice, vs 9.39 cmH_2O/ml in LB mice,

P= 0.029), and tissue elastance (57.55 ml/cmH_2O in *Ctsb*$^{-/-}$ mice, vs 124.6 ml/cmH_2O in LB mice, P= 0.026) usually observed in LB development (**Figure 4b**). In support, left lungs from *Ctsb*$^{-/-}$ showed mild signs of fibrosis in peribronchial areas (**Figure 4c**) and all over the lung tissue (**Figure 4d**), compared to the LB mice. Furthermore, *Ctsb*$^{-/-}$ mice revealed reduced septal collagen and inflammation (**Figure 4e, f**). Most importantly, genetic deletion of CatB did not affect macrophage infiltration into the lung (**Figure 4g, h**), indicating that the absence of CatB has only a direct impact on macrophage function after LTx. Taken together, these data demonstrate that a mismatched transplantation induced aberrant collagen deposition and lung dysfunction *in-vivo* via CatB, that are prevented in *Ctsb*$^{-/-}$ mice.

Macrophage-derived Cathepsin B promotes fibroblast activation

CatB-positive macrophages significantly increased in areas affected by fibrosis. To better address the molecular function of CatB, we stimulated macrophages towards a pro-inflammatory, M1, or anti-inflammatory, M2 phenotype *in-vitro* (**Figure 5a**). M1, but not M2-polarized macrophages showed a significant increase of CatB gene expression after 24h of stimulation (**Figure 5b**). Similarly, CatB activity showed a substantial increase in the medium of M1-macrophages (**Figure 5c**). Likewise, in our murine LB model, CatB expression was observed in M1-macrophages but not in M2-macrophages (**Figure 5d**). Interestingly, M1 macrophage-cytokines were previously shown increased into the BALF of BOS patients [30]. We furthermore investigated the polarization of macrophages in our mouse model of LTx, by staining and quantifying the left lung tissue for NOS2 (M1 marker) and CD206 (M2 marker). Importantly, M1 and M2-macrophage numbers increased in our model of LB, 2 months after LTx, when compared to control mice (46 NOS2+ cells in LB mice, vs 25 NOS2+ cells in Ctrl mice, P= 0.2) (**Suppl. Fig 5 a, b**), and (53 CD206+ cells in LB mice, vs. 28 CD206+ cells in Ctrl mice, P=0.16) (**Suppl. Fig 5 c, d**). Since macrophages represent the main

source of TGF-β1 [31] we analyzed the expression of *Tgfb1* and confirmed a significant increase in M1-polarized macrophages (**Figure 5e**). Interestingly, pre-treatment of M1 macrophages with a CatB-specific inhibitor (CA074) (**Figure 5f**), resulted in the impaired processing of pro-TGF-β1 (**Figure 5g**). To further confirm the direct involvement of CatB in fibrosis, we treated fibroblasts with M1-derived cell medium. Strikingly, fibroblasts showed a significant increase of TGF-β1 signaling activation, mediated by CatB activation (**Figure 5h**). Taken all together, our data demonstrates that increased activity of pro-inflammatory macrophage-derived CatB, resulted in the activation of fibroblasts driving BOS progression.

Discussion

Differently from all other proteases, Cathespin B (CatB) is able to act as exopeptidase and as endopeptidase, and exerts its activity under acidic and neutral pH conditions [32]. Its activity is broad, targeting highly similar substrates [33]. CatB expression was shown to be associated with many fibrotic diseases [13-15], however its contribution has not yet investigated in the contest of BOS. Therefore, we investigated the impact of CatB to the progression of BOS. For the first time, we demonstrated that 1) CatB activity and expression are increased in BOS patients; 2) this negatively correlates with lung function; 3) infiltrating, recipient-derived macrophages are the main source of CatB; 4) CatB activity leads to collagen production and 5) resulted in a TGF-β1-dependent activation of fibroblasts.

Although histological features of BOS are defined during the later stages of disease, the main triggers that promote BOS development have not been identified. One of the major reasons for this scientific gap is the limitation of human samples for research and the lack of a reproducible animal model of BOS combined to the technical challenges of LTx. Translational studies are restricted to BALF and peripheral blood. Surveillance bronchoscopy, including BAL and transbronchial biopsy (TBB) collection, is part of the routine follow up in our center. Lung tissue collected by TBB was however not routinely stored in our bioarchive, making it impossible for us to directly compare BAL and TBB at each given time-point. Only lung tissue samples from patients at a very late stage of the disease could be used in this study, limiting histological investigations at early time-points. This limitation makes it difficult to investigate early events that can trigger disease progression. Here, we used BALF samples that were collected at different–stages of the disease (BOS 0-3). This, coupled with our LTx mouse model of LB, enabled us to identify potential drivers of the disease.

We demonstrated a substantial increase of CatB activity in the BALF of BOS patients, starting already at BOS stage-0. In accordance with our finding, Kasabova et al. showed a marked increase of CatB activity in BALF samples of mice, during the acute phase of bleomycin-induced fibrosis, prompting the involvement of CatB in fibrosis [13]. Additionally, the expression of CatB increased over the disease progression in BOS patients and in our mouse model of LB. This observation is comparable to previous studies performed in samples from patients and mice suffering from advanced liver fibrosis [15]. In order to understand the role of CatB, we first investigated the main source in BOS. One hallmark of BOS is the influx of macrophages [32] into the allograft, in areas surrounding the airways and vessels [2]. Vasiljeva et al. demonstrated infiltrating macrophages being the source of CatB, which promoted tumor invasiveness, suggesting CatB as a main player in tumor progression [34]. Similarly, we showed that recipient monocyte-derived macrophages, that were infiltrating areas affected by collagen deposition, were the main source of CatB in BOS patients as well as in LB mice. Furthermore, we were able to characterize the subclass of CatB-producing macrophages being predominantly pro-inflammatory macrophages, which we could confirm *in-vivo* in the lungs of LB mice.

Previous studies demonstrated that LB lung tissue was characterized by a marked increase of infiltrating cells in fibrotic areas, surrounding distal airways [8] vessels and alveolar space [5, 19]. The most striking finding in our study is the observation of significant changes in disease-related factors in a time-dependent manner. Here, we showed that CatB activity as well as pro-collagen levels in BALF negatively correlated with the lung function in patients after transplantation. Interestingly, the increase of CatB activity was positively associated with the increased collagen levels detected in BALF. The increased levels of pro-collagen 1a1 were already reported as a result of fibroblast proliferation of alveolar epithelial cells [35] as well as in the BALF of patients with interstitial lung disease [36]. We found that the increase of CatB activity occurs at an early stage of

BOS disease (BOS stage 0), which is associated with an early increase of pro-collagen 1a1 synthesis (BOS stage 1). Thus, our finding in BOS patients may have additional implications in the context of biomarkers for the early diagnosis of BOS development. Strikingly, CatB-deficiency resulted in reduced collagen production, protecting the graft against the development of LB. We could definitively demonstrate that the exclusive lack of CatB was sufficient to prevent LB development. The microsurgery of LTx represents the major challenge in the experimental number of mice used in this study. However, the homogeneity of our readouts offered a clear and convincing understanding of the phenotype.

Molecularly, we could successfully demonstrate the role of CatB in regulating TGF-β1 signaling in fibroblasts leading to the progression of BOS. Previously, the increase of TGF-β1 levels was reported in the BALF from RAS patients, which was associated with a pro-fibrotic phenotype (reduced E-cadherin expression and an increased expression of α-SMA proteins) in RAS lung tissue [37]. In agreement with our findings, a previous study revealed that the increased levels of TGF-β1 were associated with the development of OB, and was also showed that the elevated expression of TGF-β1 preceded the development of OB [16]. These findings suggest that BOS and RAS lung tissue might share some common molecular features, likely in association with distinct pathways, which lead to different histological findings and clinical symptoms. The association of CatB in TGF-β1 driven activation of fibroblasts was reported *in-vitro* studies using fibroblasts from IPF patients [13] . Although, CatB expression in kidney epithelial cells was shown to negatively regulate TGF-β1 signaling, the authors already pointed to a cell-type, and disease state specific function of CatB [38]. When we addressed the role of macrophage-derived-CatB in BOS, we found that CatB was necessary to activate latent TGF-β1, and pro-inflammatory macrophages were the main source of CatB and of TGF-β1. Similar to a recent study, we demonstrated that pro-inflammatory macrophages induced fibroblast activation [39]. Furthermore, BOS patients have shown high

incidence of bacterial infection, described as source of LPS [40] and of IFNγ [41], that together could promote macrophage differentiation towards a pro-inflammatory phenotype in BOS. Strikingly, *in-vitro* inhibition of CatB activity resulted in the prevention of fibroblast activation. This finding already suggests CatB inhibition as a therapeutic target in the treatment of BOS. Based on a detailed analysis of CatB activity in our cohorts as well as in independent single cell analysis [26-28], we demonstrated a clear association between decreased levels of CysC and increased CatB activity in patients with a history of pulmonary fibrosis. We believe that there is a high systemic bioavailability of CatB in those patients which, associated with an increased recruitment of pro-inflammatory $CatB^{+}$ macrophages in the graft after LTx, results in an increase in CatB activity in BALF. Consistently, the association of CatB expression and fibrotic diseases has been widely investigated. Previous studies reported a significant increase of CatB in lung [13] as well as in liver fibrosis [15]. Analysis of a larger number of BALF samples from patients with other underlying lung diseases other than LF will be crucial to validate the significance of CatB activity in the specific of underlying LF. In the light of the increasing demand of personalized medicine, future follow-ups in a larger cohort would be needed to consider the usage of a CatB inhibitor as BOS therapy in LTx patients with a history of lung fibrosis.

In conclusion, based on our findings in human as well as in mice, this study clearly demonstrates a crucial role of macrophage-released CatB in the TGF-β1-mediated biosynthesis of collagen by fibroblasts already at early stages of the disease, suggesting CatB as early marker of BOS progression. We would like strongly suggest–CatB as–a novel potential therapeutic target in the treatment of BOS.

Figure legends

Figure Legend 1

Cathepsin B and Collagen expression increase in bronchiolitis obliterans syndrome

a, b) Quantification of secreted pro-collagen 1a1 via ELISA in bronchoalveolar lavage fluid (BALF), from Stable LTx patients (n=15), who never developed signs of bronchiolitis obliterans syndrome, and from BOS patients, who developed bronchiolitis obliterans syndrome. BALF was collected at different stages of the disease, according to the rate of FEV_1 % decline, into BOS-0 (n=5); BOS-1 (n=13); BOS-2 (n=13); BOS-3 (n=15); c) Linear correlation between pro-collagen 1a1 secreted in BALF and FEV_1 % of Stable LTx and BOS patients; BOS-0 patients are excluded for the analysis cause of no change in FEV_1 % ; d, e) Quantification of Cathepsin B (CatB) activity in human BALF via a FRET-probe based activity assay adding 10µM of Z-Arg-Arg-AMC substrate to the reaction buffer. CatB concentration was measured with serial dilutions of CatB recombinant protein; BALF was collected at different stages of the disease, according to the % decline in FEV_1 % values of baseline, into BOS-0 (n=20); BOS-1 (n=11); BOS-2 (n=12); BOS-3 (n=20); f) Linear correlation between CatB activity and its related FEV_1% value; g) Evaluation of CatB and pro-collagen 1a1 expression over BOS progression (+/- SEM); h, i) Representative Western blots of human BALF samples from Stable LTx and BOS patients. Pro-forms and mature forms of CatB were determined and quantified according to the expected molecular weight. j) Representative histological sections of bronchiolar and alveolar epithelium are shown at low (scale bar of 500µm) and high (scale bar of 100µm) magnification to illustrate the different expression and localization of CatB (top panel). Paraffin-embedded lung tissue was obtained from healthy donors (HD) and from BOS stage-3 patients; k) Representative pictures of human lung tissue stained for inflammation and for collagen

via Masson trichrome staining. Bar graphs represent mean values +/- SD. Statistical significance was assessed using Mann-Whitney U test (*P< 0.05; **P< 0.005; ***P< 0.0001) (a, b, d, e, I).

Figure legend 2

Cathepsin B is expressed in macrophages infiltrating airway-surrounding areas during BOS

a) Representative immunofluorescence staining of Cathepsin B (red), and of macrophage, Galectin 3 (green) in human lung tissue from healthy donors (HD) and BOS stage-3 patients (scale bar of 50 µm), b) Representative immunofluorescence staining of Cathepsin B (red) and of macrophage, Galectin-3 (green) (scale bar of 50 µm) 2 months after LTx in left lungs from B6→B6 (n= 4) and HLA→B6 (n= 4); c) Quantification of Galectin-3 positive cells in 20 randomly selected fields of view (FOV); d) Quantification of Cathepsin B positive cells in 20 randomly selected fields of view; e) Representative immunofluorescence staining of Cathepsin B (green) and left lung donor-derived antigen, HLA.A2 (red) in lung tissue from HLA→ B6, 2 months after LTx. Values were normalized to the total area. Violin plots represent mean values. Statistical significance was assessed using Mann-Whitney U test (*P< 0.05; **P< 0.005) (c, d).

Figure legend 3

Cathepsin B expression in an orthotopic murine model of LB

a) Experimental design of a time-course orthotopic murine left lung transplantation (LTx) model; b) Representative pictures of murine lung tissue stained for inflammation and for collagen via Masson trichrome staining (scale bar of 200µm); c) Quantification of collagen and inflammation in lung tissue was performed via a computer-assisted stereology analysis (CAST) around airways, vessels, and septal area. Values are represented as mean values, and expressed as volume on surface

(µm3/µm2); d) Representative immunofluorescence staining of Cathepsin B in lung tissue (scale bar of 50µm); e) Representative western blots of Cathepsin B, collagen 1 and fibronectin 1 (FN1) expression in lung tissue lysate, and f) in BALF. Equal amount of total protein was loaded for lung tissue analysis (15 µg), and equal volume was loaded for BALF analysis. Pro-forms and mature forms of Cathepsin B were detected according to the molecular weight.

Figure legend 4

Genetic deletion of Cathepsin B protects lung grafts from LB

a) Experimental design of orthotopic left lung transplantation (LTx) in CatB knock-out mice (*Ctsb*-/-). Left lungs from non-transplanted HLA.A2 mice were used as control (Ctrl), for which the lung function has been measured after clamping the right bronchus, as for the transplanted mice. b) *In-vivo* measurements of left lung function via Flexivent, 28 days after LTx. Right bronchi were clamped during the entire time of lung function measurements. Measurements were normalized to the body weight of the recipient mouse; c) Evaluation of inflammation and collagen deposition was determined via Masson trichrome staining of left lung tissue, 28 days after LTx. Representative pictures are shown for each group, at low magnification (1000µm, left panel), and high magnification (100 µm, right panel); d-f) Quantification of inflammation and collagen of left lung tissue, in areas surrounding airways, vessel and septum, was performed via computer-assisted stereology (CAST); g) Quantification of macrophages in left lung tissue at 28 days after LTx via computer-assisted stereology (CAST). Representative pictures of macrophage immunostaining, positive for Galectin-3 (scale bar of 50µm); h) Quantification of macrophage in left lung tissue. Violin plots represent mean values =/- SD. Statistical significance was assessed using one-way ANOVA, Kruskal Wallis (*P< 0.05; **P< 0.005; ***P< 0.0003; ****P< 0.0001).

Figure legend 5

Cathepsin B contributes to fibroblast activation via TGF-β1ß -maturation

a) Experimental design of macrophage (Raw264.7) differentiation with IFN-γ (20 ng/ml) and LPS (1 µg/ml), IL-4 (20 ng/ml) or medium alone. Macrophage cell supernatant was used to analyze Cathepsin B (CatB) activity, active TGF-β1 levels, and for further treatment of fibroblasts (MEF). Macrophage cell lysate was used for gene expression analysis; b) gene expression analysis of murine CatB in macrophages at different times of differentiation; c) quantification of CatB activity in cell supernatant via FRET-based activity assay; d) Representative immunofluorescence staining of CatB (green) and NOS2 (red) expression (upper panel), and of CatB (red) and CD206 (green) (lower panel), in a murine model of LB(scale bar of 10µm); e) Gene expression analysis of murine tgfb1 in macrophages at different times of differentiation; f) Quantification of CatB activity in cell supernatant of macrophage-pretreated with CA074 (10µM), or DMSO, and stimulated for 24h or 48h with IFN-γ (20 ng/ml) and LPS (1 µg/ml) via FRET-based activity assay; g) Quantification of active TGF-β1 in cell supernatant of macrophage-pretreated with CA074 (10µM), or DMSO, and stimulated for 24h and 48h with IFN-γ (20 ng/ml) and LPS (1 µg/ml) via ELISA; h) Quantification of pSMAD3 signal in MEF cells after 30 minutes of stimulation with macrophage-conditioned medium (CM) via Western blot. Macrophages were pre-treated with CA074 (10µM) or DMSO, then stimulated for 24h with IFN-γ (20 ng/ml) and LPS (1 µg/ml). Cell supernatant was collected, centrifuged and add to starved fibroblasts (n=2, N=3). Western blot signals were normalized to β-actin, and internal controls. Violin plots represent mean values +/- SD. Statistical significance was assessed using\One-way ANOVA, Kruskal Wallis (b, c, e., f, g) and Turkey´s multiple test (h) (*P< 0.05; **P< 0.005; ***P< 0.0003; ****P< 0.0001).

Acknowledgments: The authors are thankful to Prof. Fernando Holguin from the University of Colorado Denver, for his support in the statistic analysis of human data; Thomas M Conlon for editing the manuscript; to Salome Rehm for her prompt help in ordering materials; to the Hospital Marie-Lannelongue, Le Plessis-Robinson, France, for providing the human BOS-Stage 3 lung tissue, and to CPC-BioArchive for providing Stable lung resections (Healthy donors, HD) from non-transplanted donors lung tissue.

Support statement: This was supported by the German Center for Lung Research (DZL); by the European Union's Horizon 2020 Research and Innovation Program (668036, RELENT) and Max-Planck-Society.

References

1. Meyer KC. Recent advances in lung transplantation. *F1000Res* 2018; 7.
2. Estenne M, Hertz MI. Bronchiolitis obliterans after human lung transplantation. *Am J Respir Crit Care Med* 2002; 166: 440-444.
3. Kulkarni HS, Cherikh WS, Chambers DC, et al. Bronchiolitis obliterans syndrome-free survival after lung transplantation: An International Society for Heart and Lung Transplantation Thoracic Transplant Registry analysis. *J Heart Lung Transplant* 2019; 38: 5-16.
4. Estenne M, Maurer JR, Boehler A, et al. Bronchiolitis obliterans syndrome 2001: an update of the diagnostic criteria. *J Heart Lung Transplant* 2002; 21: 297-310.
5. Weigt SS, DerHovanessian A, Wallace WD, et al. Bronchiolitis obliterans syndrome: the Achilles' heel of lung transplantation. *Semin Respir Crit Care Med* 2013; 34: 336-351.
6. Stewart S, Fishbein MC, Snell GI, et al. Revision of the 1996 working formulation for the standardization of nomenclature in the diagnosis of lung rejection. *J Heart Lung Transplant* 2007; 26: 1229-1242.
7. Verleden SE, Vos R, Vanaudenaerde BM, et al. Chronic lung allograft dysfunction phenotypes and treatment. *J Thorac Dis* 2017; 9: 2650-2659.
8. Colom AJ, Teper AM. Post-infectious bronchiolitis obliterans. *Pediatr Pulmonol* 2019; 54: 212-219.
9. Jaramillo A, Fernandez FG, Kuo EY, et al. Immune mechanisms in the pathogenesis of bronchiolitis obliterans syndrome after lung transplantation. *Pediatr Transplant* 2005; 9: 84-93.
10. Meng XM, Nikolic-Paterson DJ, Lan HY. TGF-beta: the master regulator of fibrosis. *Nat Rev Nephrol* 2016; 12: 325-338.
11. Mu D, Cambier S, Fjellbirkeland L, et al. The integrin alpha(v)beta8 mediates epithelial homeostasis through MT1-MMP-dependent activation of TGF-beta1. *J Cell Biol* 2002; 157: 493-507.
12. Sun B, Zhou Y, Halabisky B, et al. Cystatin C-cathepsin B axis regulates amyloid beta levels and associated neuronal deficits in an animal model of Alzheimer's disease. *Neuron* 2008; 60: 247-257.
13. Kasabova M, Joulin-Giet A, Lecaille F, et al. Regulation of TGF-beta1-driven differentiation of human lung fibroblasts: emerging roles of cathepsin B and cystatin C. *J Biol Chem* 2014; 289: 16239-16251.
14. Kasabova M, Villeret B, Gombault A, et al. Discordance in cathepsin B and cystatin C expressions in bronchoalveolar fluids between murine bleomycin-induced fibrosis and human idiopathic fibrosis. *Respir Res* 2016; 17: 118.
15. Manchanda M, Das P, Gahlot GPS, et al. Cathepsin L and B as Potential Markers for Liver Fibrosis: Insights From Patients and Experimental Models. *Clin Transl Gastroenterol* 2017; 8: e99.
16. El-Gamel A, Sim E, Hasleton P, et al. Transforming growth factor beta (TGF-beta) and obliterative bronchiolitis following pulmonary transplantation. *J Heart Lung Transplant* 1999; 18: 828-837.
17. Kneidinger N, Milger K, Janitza S, et al. Lung volumes predict survival in patients with chronic lung allograft dysfunction. *Eur Respir J* 2017; 49.
18. Smirnova NF, Conlon TM, Morrone C, et al. Inhibition of B cell-dependent lymphoid follicle formation prevents lymphocytic bronchiolitis after lung transplantation. *JCI insight* 2019; 4.

19. Muller C, Andersson-Sjoland A, Schultz HH, et al. Early extracellular matrix changes are associated with later development of bronchiolitis obliterans syndrome after lung transplantation. *BMJ Open Respir Res* 2017; 4: e000177.
20. Verleden GM, Glanville AR, Lease ED, et al. Chronic lung allograft dysfunction: Definition, diagnostic criteria, and approaches to treatment-A consensus report from the Pulmonary Council of the ISHLT. *J Heart Lung Transplant* 2019; 38: 493-503.
21. Lammi L, Ryhanen L, Lakari E, et al. Type III and type I procollagen markers in fibrosing alveolitis. *Am J Respir Crit Care Med* 1999; 159: 818-823.
22. Westra IM, Mutsaers HA, Luangmonkong T, et al. Human precision-cut liver slices as a model to test antifibrotic drugs in the early onset of liver fibrosis. *Toxicol In Vitro* 2016; 35: 77-85.
23. Montesi SB, Izquierdo-Garcia D, Desogere P, et al. Type I Collagen-targeted Positron Emission Tomography Imaging in Idiopathic Pulmonary Fibrosis: First-in-Human Studies. *Am J Respir Crit Care Med* 2019; 200: 258-261.
24. Kim YI, Shin HW, Chun YS, et al. Epithelial cell-derived cytokines CST3 and GDF15 as potential therapeutics for pulmonary fibrosis. *Cell Death Dis* 2018; 9: 506.
25. Sokol JP, Neil JR, Schiemann BJ, et al. The use of cystatin C to inhibit epithelial-mesenchymal transition and morphological transformation stimulated by transforming growth factor-beta. *Breast Cancer Res* 2005; 7: R844-853.
26. Adams TS, Schupp JC, Poli S, et al. Single-cell RNA-seq reveals ectopic and aberrant lung-resident cell populations in idiopathic pulmonary fibrosis. *Sci Adv* 2020; 6.
27. Morse C, Tabib T, Sembrat J, et al. Proliferating SPP1/MERTK-expressing macrophages in idiopathic pulmonary fibrosis. *Eur Respir J* 2019; 54.
28. Habermann AC, Gutierrez AJ, Bui LT, et al. Single-cell RNA sequencing reveals profibrotic roles of distinct epithelial and mesenchymal lineages in pulmonary fibrosis. *Sci Adv* 2020; 6: eaba1972.
29. Sottile J, Hocking DC. Fibronectin polymerization regulates the composition and stability of extracellular matrix fibrils and cell-matrix adhesions. *Mol Biol Cell* 2002; 13: 3546-3559.
30. Borthwick LA, Corris PA, Mahida R, et al. TNFalpha from classically activated macrophages accentuates epithelial to mesenchymal transition in obliterative bronchiolitis. *Am J Transplant* 2013; 13: 621-633.
31. Wynn TA, Barron L. Macrophages: master regulators of inflammation and fibrosis. *Semin Liver Dis* 2010; 30: 245-257.
32. Leonard CT, Soccal PM, Singer L, et al. Dendritic cells and macrophages in lung allografts: A role in chronic rejection? *Am J Respir Crit Care Med* 2000; 161: 1349-1354.
33. Vidak E, Javorsek U, Vizovisek M, et al. Cysteine Cathepsins and their Extracellular Roles: Shaping the Microenvironment. *Cells* 2019; 8.
34. Vasiljeva O, Papazoglou A, Kruger A, et al. Tumor cell-derived and macrophage-derived cathepsin B promotes progression and lung metastasis of mammary cancer. *Cancer Res* 2006; 66: 5242-5250.
35. Keane MP, Donnelly SC, Belperio JA, et al. Imbalance in the expression of CXC chemokines correlates with bronchoalveolar lavage fluid angiogenic activity and procollagen levels in acute respiratory distress syndrome. *J Immunol* 2002; 169: 6515-6521.
36. King TE, Jr., Mortenson RL. Bronchoalveolar lavage in patients with connective tissue disease. *J Thorac Imaging* 1992; 7: 26-48.
37. Sacreas A, von der Thusen JH, van den Bosch TPP, et al. The pleural mesothelium and transforming growth factor-beta1 pathways in restrictive allograft syndrome: A pre-clinical investigation. *J Heart Lung Transplant* 2019; 38: 570-579.

38. Zhang X, Zhou Y, Yu X, et al. Differential Roles of Cysteinyl Cathepsins in TGF-beta Signaling and Tissue Fibrosis. *iScience* 2019; 19: 607-622.
39. Hindman B, Ma Q. Carbon nanotubes and crystalline silica stimulate robust ROS production, inflammasome activation, and IL-1beta secretion in macrophages to induce myofibroblast transformation. *Arch Toxicol* 2019; 93: 887-907.
40. Yomota M, Yanagawa N, Sakai F, et al. Association between chronic bacterial airway infection and prognosis of bronchiolitis obliterans syndrome after hematopoietic cell transplantation. *Medicine (Baltimore)* 2019; 98: e13951.
41. Hodge G, Hodge S. Therapeutic Targeting Steroid Resistant Pro-Inflammatory NK and NKT-Like Cells in Chronic Inflammatory Lung Disease. *Int J Mol Sci* 2019; 20.

Figure 1

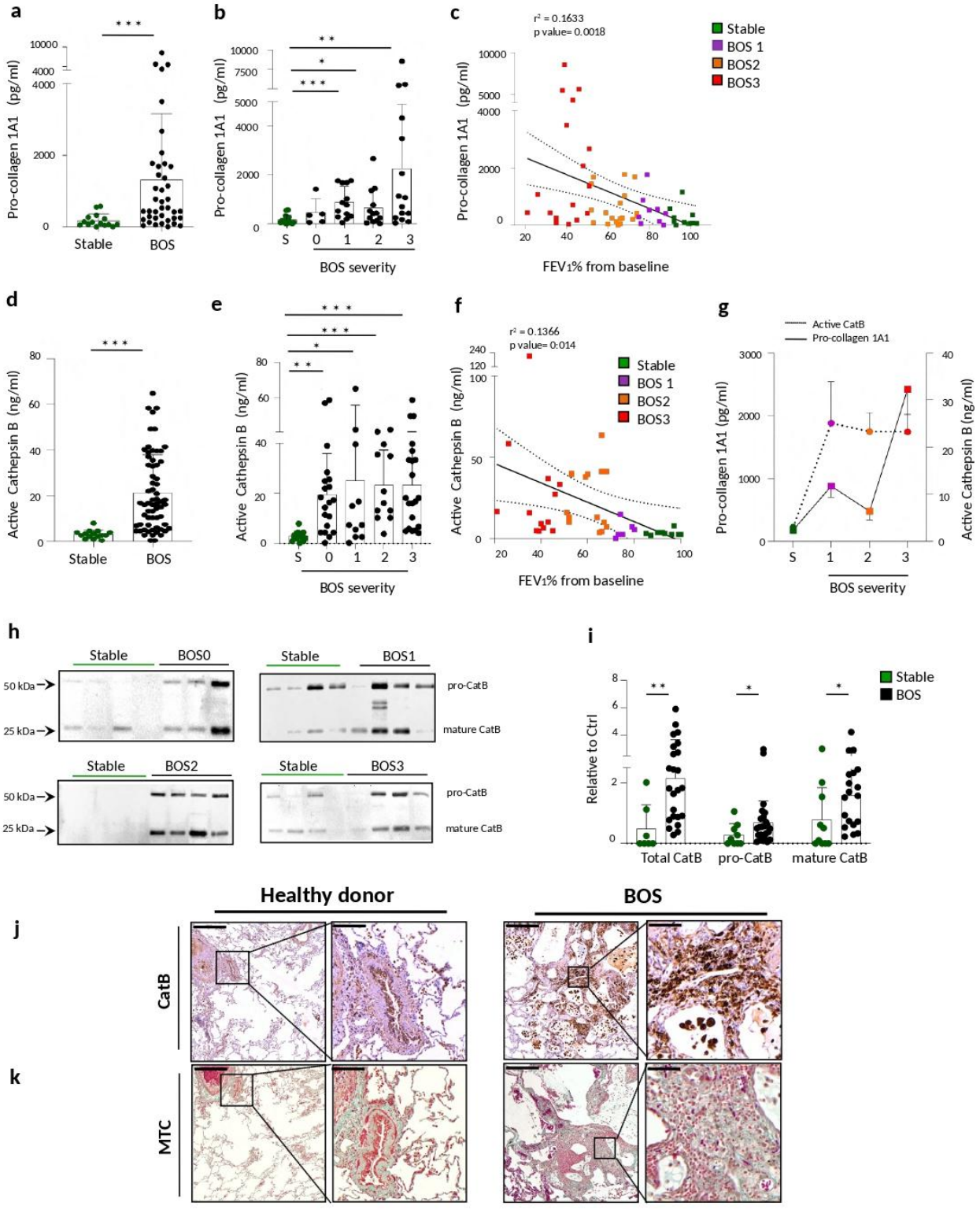
a
b
c
Pro-collagen 1A1 (pg/ml)
Stable
BOS
BOS severity
FEV1% from baseline
r² = 0.1633
p value= 0.0018
Stable
BOS 1
BOS2
BOS3
d
e
f
g
Active Cathepsin B (ng/ml)
r² = 0.1366
p value= 0.014
Active CatB
Pro-collagen 1A1
h
Stable
BOS0
BOS1
BOS2
BOS3
50 kDa
25 kDa
pro-CatB
mature CatB
i
Relative to Ctrl
Total CatB
pro-CatB
mature CatB
Healthy donor
BOS
j
CatB
k
MTC

Figure 2

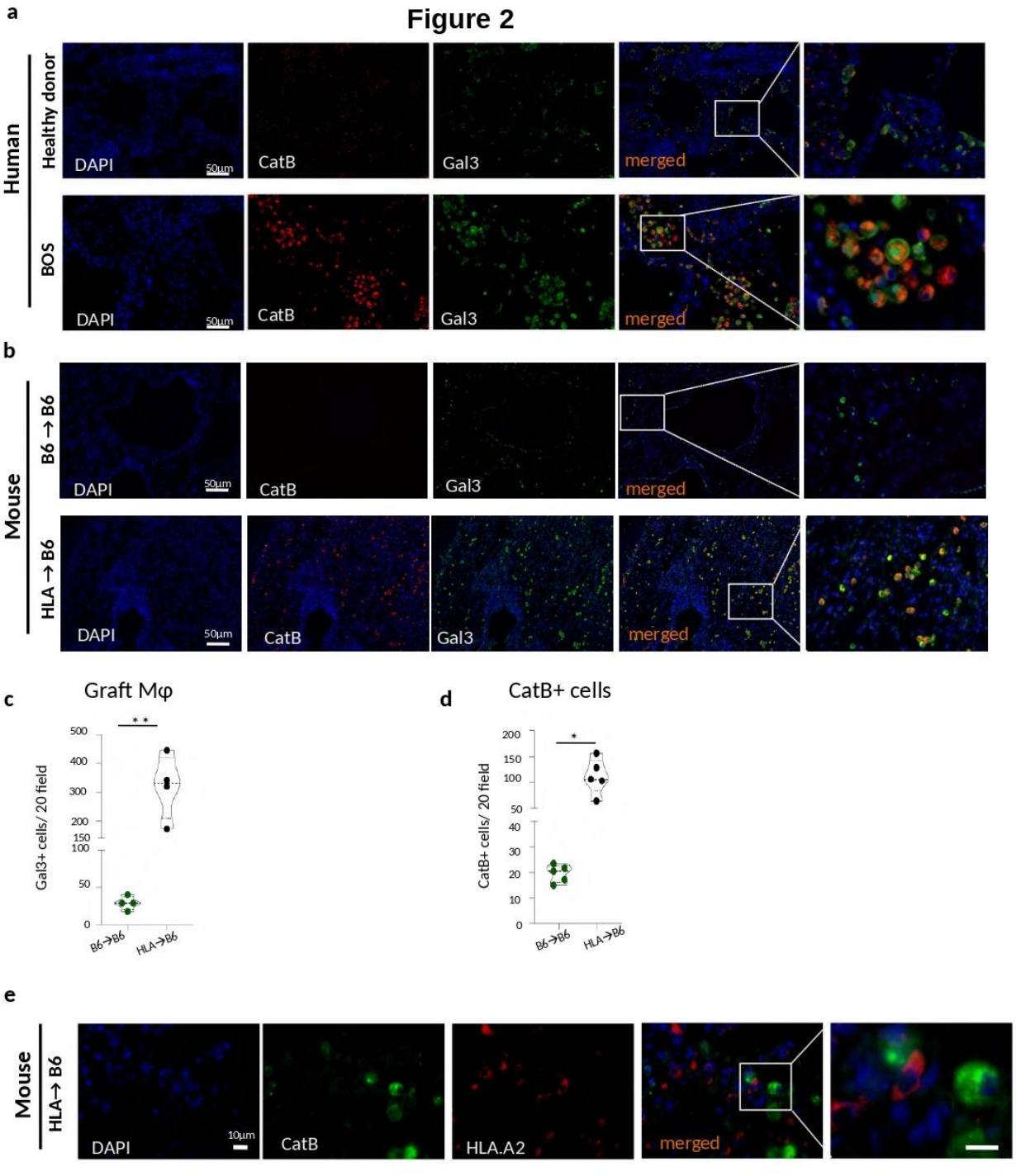
a
Human
Healthy donor
BOS
DAPI
50μm
CatB
Gal3
merged
b
Mouse
B6 → B6
HLA → B6
c
Graft Mφ
Gal3+ cells/ 20 field
B6→B6
HLA→B6
d
CatB+ cells
CatB+ cells/ 20 field
e
Mouse
HLA→ B6
10μm
HLA.A2

Figure 3

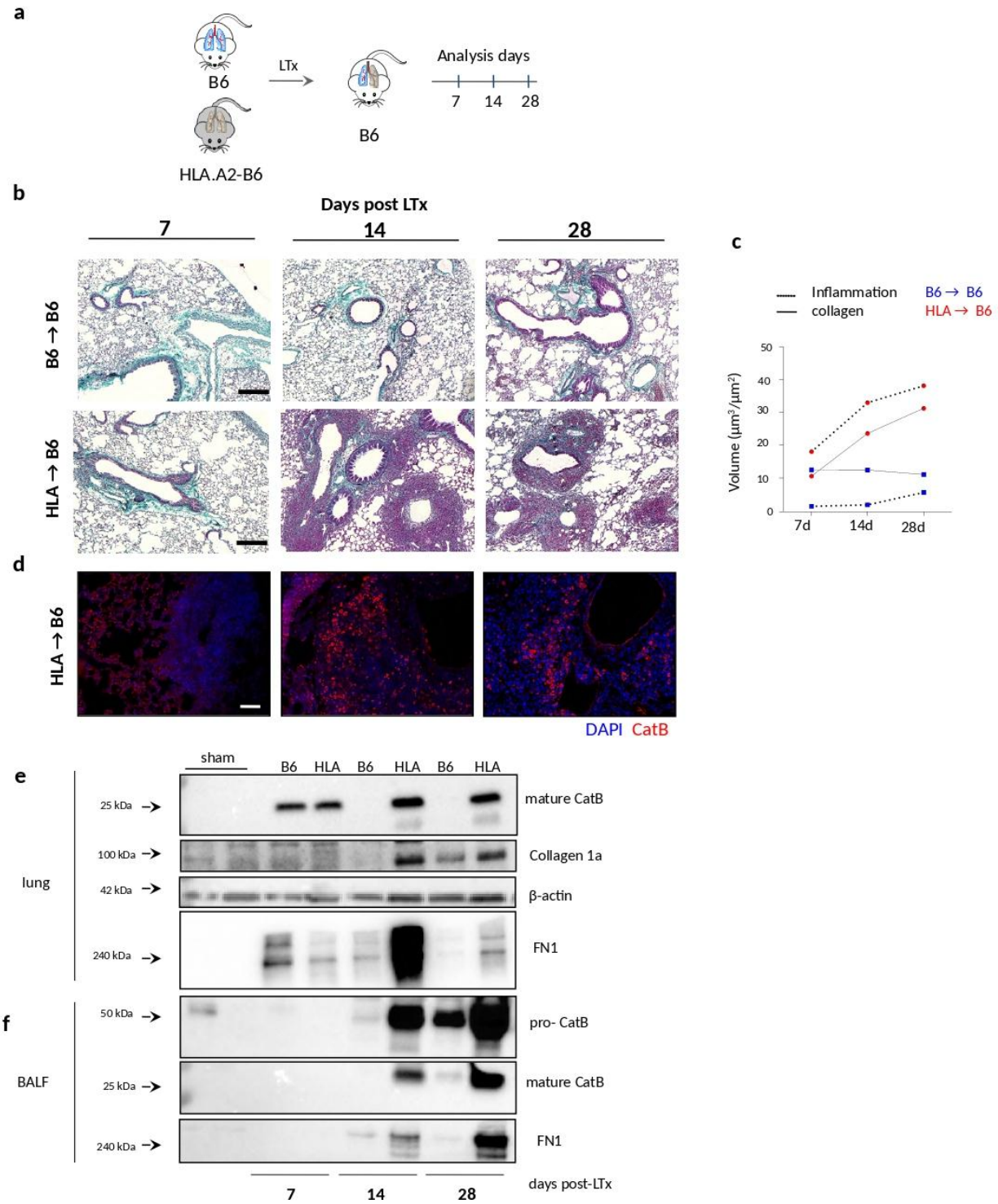
a
B6
HLA.A2-B6
LTx
B6
Analysis days
7 14 28
b
Days post LTx
7
14
28
B6 → B6
HLA → B6
c
Inflammation
collagen
B6 → B6
HLA → B6
Volume (µm³/µm²)
50
40
30
20
10
0
7d
14d
28d
d
HLA → B6
DAPI CatB
e
sham
B6 HLA B6 HLA B6 HLA
lung
25 kDa
100 kDa
42 kDa
240 kDa
mature CatB
Collagen 1a
β-actin
FN1
f
BALF
50 kDa
25 kDa
240 kDa
pro- CatB
mature CatB
FN1
7 14 28
days post-LTx

Figure 4

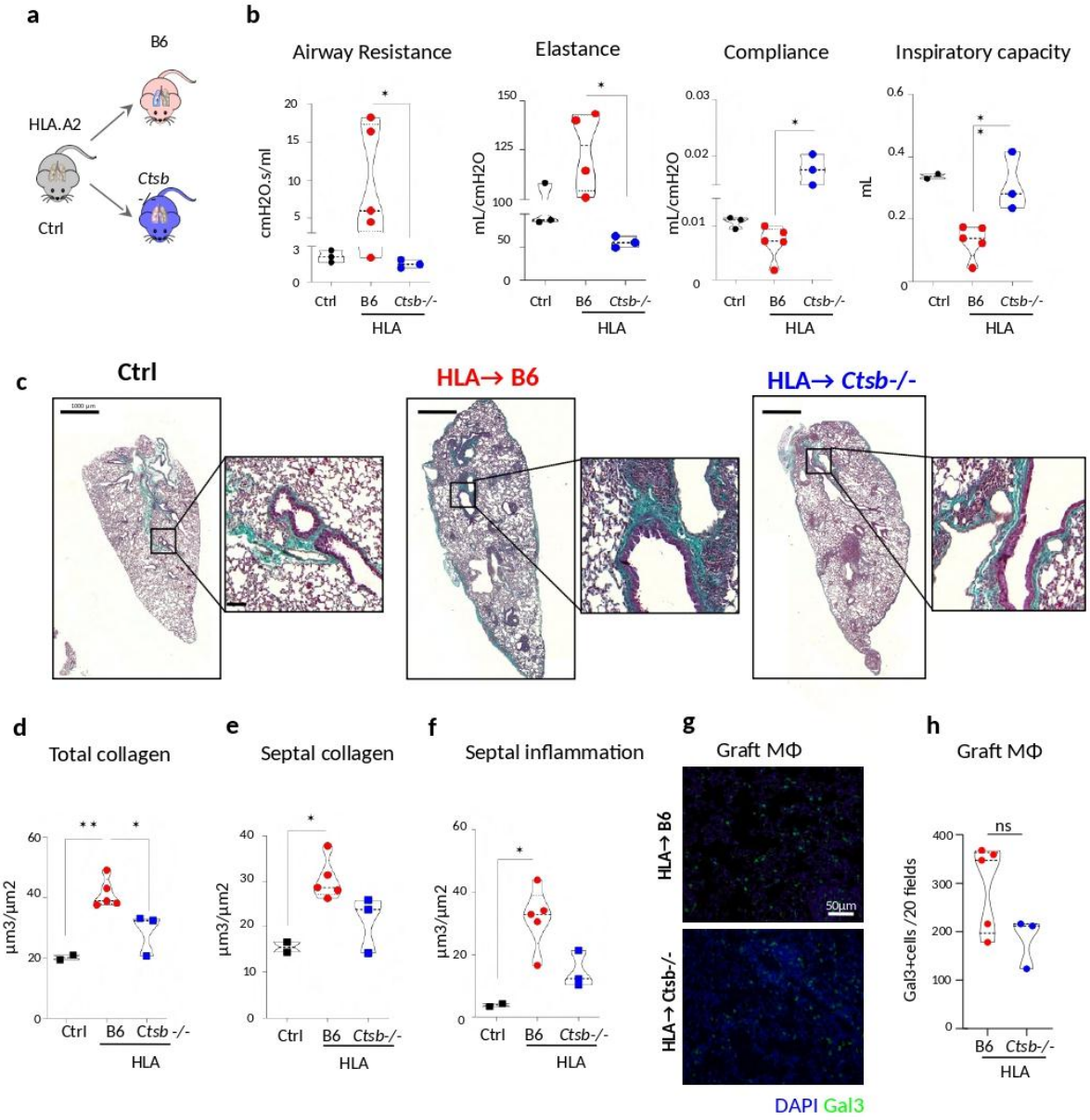
a
B6
HLA.A2
Ctsb -/-
Ctrl
b
Airway Resistance
cmH2O.s/ml
Elastance
mL/cmH2O
Compliance
mL/cmH2O
Inspiratory capacity
mL
Ctrl
B6
Ctsb-/-
HLA
c
Ctrl
HLA→ B6
HLA→ Ctsb-/-
d
Total collagen
µm3/µm2
e
Septal collagen
µm3/µm2
f
Septal inflammation
µm3/µm2
g
Graft MΦ
HLA→ B6
HLA→ Ctsb-/-
50µm
DAPI Gal3
h
Graft MΦ
Gal3+cells /20 fields
ns

Figure 5

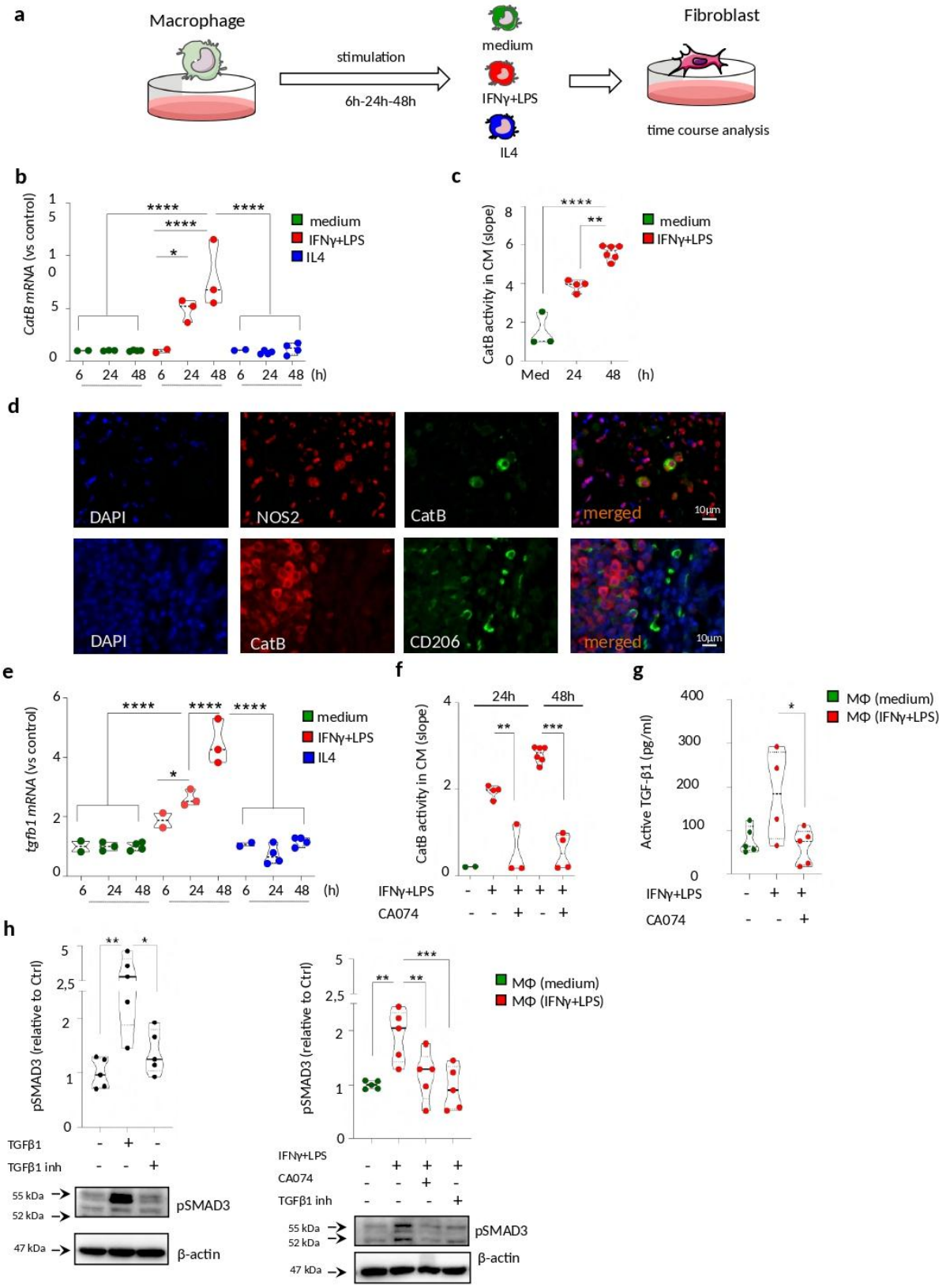
a
Macrophage
stimulation
6h-24h-48h
medium
IFNγ+LPS
IL4
Fibroblast
time course analysis
b
CatB mRNA (vs control)
medium
IFNγ+LPS
IL4
6 24 48 6 24 48 6 24 48 (h)
c
CatB activity in CM (slope)
Med 24 48 (h)
d
DAPI
NOS2
CatB
merged
CD206
10µm
e
tgfb1 mRNA (vs control)
f
24h
48h
IFNγ+LPS
CA074
g
Active TGF-β1 (pg/ml)
MΦ (medium)
MΦ (IFNγ+LPS)
h
pSMAD3 (relative to Ctrl)
TGFβ1
TGFβ1 inh
55 kDa
52 kDa
47 kDa
pSMAD3
β-actin

Supplemental Information

Cathepsin B promotes collagen biosynthesis driving Bronchiolitis Obliterans Syndrome

Carmela Morrone, Natalia F. Smirnova, Aicha Jeridi, Nikolaus Kneidinger, Christine Hollauer, Jonas Christian Schupp, Naftali Kaminski, Dieter Jenne, Oliver Eickelberg, and Ali Önder Yildirim.

Material and Method

Human patient descriptions

All patients in our center undergo routinely body plethysmography at every visit as part of the structured follow-up. In this context, we recently published a detailed description of our entire bilateral lung transplant cohort, with a focus on physiological phenotypes, such as air entrapment (hyperinflation) and restriction (rigidity) and their combination (mixed)[1] . In the current analysis only patients with a definite BOS phenotype were selected. BOS was defined as an isolated obstructive phenotype (FEV_1/FVC ratio <0.70, i.e. without a concomitant and persistent decrease of total lung capacity (TLC) ($TLC/TLC_{baseline}$ <90%)) and without persistent radiologic pulmonary opacities, which is in line with previous and current consensus definitions [2, 3] .

Human BAL collection

BAL collection was performed with the fiberoptic bronchoscope by specialized clinical personnel. A total volume of 100 ml of saline solution was instilled, and the sample was then retracted. The volume of retrieved BAL was recorded. The BAL sample was centrifuged and BAL pellet was separated from the BAL fluid (BALF). BAL pellet was used for BAL cell differential counts, while BALF was pooled in aliquots for routine analysis, and frozen at -80°C for molecular analysis [4]. BAL collection from stable BOS-3 patients was not routinely performed, since bronchoscopy in patients with end-stage BOS is associated with risks, and indication was set very carefully. BALF from BOS-0 were taken as part of surveillance bronchoscopy, 6 or 12 months after transplantation. We routinely performed bronchoscopy on Stable LTx patients at 3, 6 and 12 months and at later time points, to rule out infection or suspicious of allograft dysfunction. Patients were clinically defined stable if no infection or rejection was diagnosed and remained stable for over 5 years from the time of BAL collection. Patients undergo bronchoscopy if a clinically relevant lung function decline is noticed (e.g. BOS-2→ BOS-3) as indicated by the treating physician for differential diagnostics. Samples were only used for current analysis if other reasons than chronic rejection were excluded.

All BALFs that were used in this study were collected and stored from 2004 until 2014. For the following analysis, we selected patients with clear evidence of BOS, and patients with stable LTx from our bio-archive.

Orthotopic left lung transplantation mouse model

The mouse model used in this study, as previously reported [5], is a model of lymphocytic bronchiolitis (LB). This model clearly shows pathological changes similar to human BOS, including peribronchial mononuclear cell infiltration, ECM deposition in areas surrounding airways, selective loss of club cells, immune follicle formation, bronchiolar epithelial cell dysplasia, and epithelial undulation [6]. Our mouse model has a strong resemblance to the pre-obliterative phenotype, but lacks parenchymal fibrosis, characteristic of the restrictive phenotype [7]. Since LB is considered a precursor of OB in BOS [8, 9] our model is useful to get insights into the initiation of BOS development.

Immunohistochemistry

Sections were deparaffinized, and rehydrated with PBS-Tween 20 (0.1%), PBS-T, for 10 min. Endogenous peroxidases were quenched by incubation in 3% H_2O_2 (30%, H1009, Sigma Aldrich) in PBS for 10 min. After washing with PBS-T, avidin solution (Avidin/Biotin Blocking Kit, SP-2001; Vector Laboratories) was added and incubated for 15 min, followed by washing with PBS-T; biotin solution was added for 15 min, and washed again; sections were blocked with PBSA (BSA 3% in PBS), and incubated overnight at 4°C with the primary antibody. After washing in PBS-T, visualization was performed by incubating sections with HRP-conjugated secondary antibody for 30 min at room temperature followed by the addition of the substrate (ImmPACT DAB Peroxidase (HRP) Substrate, SK-4105; Vector Laboratories). After counterstaining with Hematoxylin, dehydration and mounting, the sections were scanned using the Axio Imager (Imager.M2, Zeiss).

Double immunofluorescence

Double immunofluorescence was performed as previously described [10]. The following primary antibodies were used in our study: anti-Gal3 (1:100, sc-20157), anti-Cystatin-C (1:200, ab109508), anti-cathepsin B (1:200, ab58802), anti-Ly6G (biolegend 127602), anti-CD45R (labome clone RA3-SB2), anti-HLA.A2 (1:200, ab52922), anti-CD206 (1:200, 18704 1-AP), anti-NOS2 (1:50, sc-8310), anti-CD45R (1:50, Labome clone RA3-SB2), anti-CD3 (1:100, Abcam clone SP7).

In vitro experiments

RAW264.7 cells were cultured with 10% FBS and 1% Pen/Strep supplemented medium, seeded at 1,5x 10^5 in 12 well-plates, and treated depending on the experimental setup. For conditioned medium (CM) preparation, RAW264.7 cells were starved for 18h (1% FBS), then pretreated for 1h with CA074 (10µM, Sigma C5732) or DMSO, and stimulated with IFNg (20ng/ml) and LPS (1µg/ml), or IL4 (20ng/ml), and TGF-β1 receptor-2 inhibitor (SB431542, 10 µM). For CM assay, CM was centrifuged at 300g x 5min at RT, and supernatant was applied on MEF cells, mouse embryonic fibroblasts, previously seeded at 5x 10^5 cells in 6 well-plates, and starved for 18 h. Fibroblast activation was evaluated after 30 min.

ELISA measurements:

Active TGF-β1 was detected in RAW264.7 CM via an ELISA kit (Bosterbio EK0515). 100µl of medium was used for each experimental condition.

Pro-collagen 1a1 detection in human BALF was performed via an ELISA kit (R&D Systems DY6220-05). Same volume of BALF (50 µl) samples was used.

Cystatin C detection in human BALF was performed via an ELISA kit (R&D System DSCTC0). Same volume of BALF (50 µl) was used.

FRET-based activity assay: Cathepsin-B activity in BALF and CM was measured fluorometrically (emission: 450 nm) using a specific Z-Arg-Arg-7-amido-4-methylcoumarin hydrochloride (10µM C429 Sigma Aldrich) substrate in 50 mM Tris, 150 mM NaCl, 0.01% Tween-20 (pH 5).

Western blot: The total protein concentration of cell, lung tissue and BALF in RIPA lysis buffer (50 mM Tris, 150 mM NaCl, 1 mM EDTA, 0.5% (w/v) deoxycholic acid, 0.1% (w/v) SDS, 0.5% (v/v) Nonidet P-40, pH 8.0) has been determined by Pierce™ BCA. Proteins were separated on 12% SDS-PAGE under denaturizing conditions, then transferred to PVDF membranes. Membranes were blocked with 1× Roti® block (Carl Roth) or 5% Milk, and incubated at 4 °C with primary antibodies–directed against CatB (1:400 ab58802) and (1:500 MAB965 R&D System); phospho-smad-3 (1:1000, cell signaling 9520); collagen 1 (1:000, Rockland 600-401-103);–fibronectin-1 (1:1000, abcam ab-2413) and β-actin (1:4000, Sigma-Aldrich A3854). The following secondary antibodies were used: anti-rabbit IgG-HRP (1:3000, 7074P2 New England Biolabs), and anti-mouse (1:3000, NA931V GE Healthcare).

RNA isolation and gene expression analysis: RNA from cells was isolated using the peqGOLD total RNA kit (Peqlab). Reverse transcription was performed using Applied Biosystem kit. Gene expression was analyzed using Platinum™ SYBR™ Green qPCR SuperMix-UDG (Thermo Fisher)

on a StepOnePlus 96 well RealTime PCR System (Applied Biosystems) and specific primer (Mouse hprt3: Fwd TCC TCC TCA GAC CGC TTT T, Rv CCTGGTTCATCATCGCTAATC; Mouse hprt2: Fwd CCT AAG ATG AGC GCA AGT TGA A, Rv CCA CAG GAC TAG AAC ACC TGC TAA; Mouse ctsb: Fwd AGCCATTTCTGACCGAACCT, TGGTAAGCAGCCTACATGAGAA; Mouse tgfβ1: Fwd TGA CGT CAC TGG AGT TGT AGT TGT ACG, GGT TCA TGT CAT GGA TGG TGC)

Supplementary Figures

Supplementary Figure 1

Demographics of patients involved in the study

a) Description of patients considered this study: BALF samples from healthy and BOS patients at different stages of the disease. BOS grade scoring was based on the analysis of the forced expiratory volume in 1 second percentage (FEV_1%) at the time of BALF collection. COPD is for chronic obstructive pulmonary disease, LF for lung fibrosis which includes idiopathic pulmonary fibrosis (IPF) and non-IPF patients, CF is for cystic fibrosis, PH is for pulmonary hypertension, DLTx is for double lung transplantation; LDH is for lactate dehydrogenase; b) Analysis of the forced expiratory volume in 1 second decline (FEV_1 %) in healthy and BOS patients used in this study; c) Analysis of total lung capacity percentage (TLC %) in healthy and BOS patients considered in this study; d) Quantification of alveolar macrophage percentage detected in BALF from healthy and BOS patients considered in this study; e) Quantification of human BALF total

protein, from healthy patients (H), who never developed signs of bronchiolitis obliterans syndrome, and from BOS patients, who developed bronchiolitis obliterans syndrome. BALF was collected at different stages of the disease, according to the rate of FEV_1 % decline, into BOS-0 (n=20); BOS-1 (n=13); BOS-2 (n=13); BOS3 (n=20); f) Description of BOS explanted lungs from re-transplanted patients considered in this study. PAH is for pulmonary arterial hypertension, IPD is for idiopathic pulmonary fibrosis, nd is for not-defined, SLTx is for single lung transplantation, DLTx is for double lung transplantation, M is for male; F is for female. Violin plots represent mean values. Statistical significance was assessed using Mann-Whitney U test (*P< 0.05; **P< 0.005; **P< 0.0001) (b, c), and one-way ANOVA (d, e).

Supplementary Figure 2

Cathepsin B activity increases in bronchoalveolar lavage fluid of BOS patients that were showing signs of lung fibrosis before LTx.

a) Representative immunofluorescence staining of Cystatin-C (CysC) in human lung tissue, from Healthy donors (HD) and BOS stage-3 patients (scale bar of 50µm); b) Quantification of CysC-positive cells in 20 fields of view (FOV) in human lung tissue; c) Representative immunofluorescence staining of Cystatin-C (red) and macrophage marker, Galectin 3 (green) in Healthy human lung tissue after LTx; d) Quantification of Cathepsin B (CatB) activity in human BALF from patients affected by lung fibrosis (LF), and e) in other underlying diseases (COPD, cystic fibrosis, CF, and pulmonary hypertension, PH) in healthy and BOS patients. CatB activity

was determined via a FRET-probe based activity assay in healthy and BOS patients; f) Quantification of Cystatin-C levels in human BALF was determined via ELISA and analyzed in healthy and BOS patients affected by lung fibrosis (LF), and g) in patients affected by other lung diseases (COPD, cystic fibrosis, CF, and pulmonary hypertension, PH). Violin plots represent mean values. Statistical significance was assessed using Mann-Whitney U test (*P< 0.05; **P< 0.005; ***P< 0.0001) (b, d, f), and one-way ANOVA (e).

Supplementary Figure 3

Macrophages are the main source of Cathepsin B in human explanted lung tissue from IPF patients.

UMAPs of mesenchymal cells labelled by cell type, disease status, and gene of interest (CTSB). Boxplot graphs represent the gene expression level of CTSB in the macrophage (M)/alveolar macrophage (AM)/ B cell (B)/ T cell (T)/ Natural killer cell (NK) population depending on the disease state. a) Combined t-distributed stochastic neighbor embedding (T-SNE) of 312,928 lung cells from 32 IPF and 28 control indicates cell types including a large central grouping of macrophage/ monocytes/ B cells/Natural killer (NK)/T cells [11]; b) Combined t-distributed stochastic neighbor embedding (t-SNE) analysis of single-cell RNA-sequencing of 70000 single-cell suspensions from 3 non-fibrotic control and 6 IPF lungs [12]; c) Combined t-distributed stochastic neighbor embedding (t-SNE) analysis of 114,396 cells identified in 31 distinct cell

types. Single-cell suspensions from peripheral lung tissue removed at the time of lung transplant surgery from patients with IPF (n=12) and no fibrotic control (n=10) [13].

Supplementary Figure 4

T and B cells do not express Cathepsin B in BOS

Left lungs from HLA-A2–knockin (HLA) mice on a B6 background (HLA) were orthotopically transplanted into B6 recipient mice and analyzed 2 months after LTx (HLA→B6, n= 4). a) Representative immunofluorescence staining of Cathepsin B (red), and neutrophils, Ly6G-positive (green) in murine BOS lung tissue, 2 months after LTx (scale bar of 50 µm); b) Representative immunofluorescence staining of Cathepsin B (red) and T-cell marker, CD3 (green) in murine BOS lung tissue, and c) B-cell marker, CD45R (green) in murine BOS lung tissue.

Supplementary Figure 5

Macrophage-polarization in the mouse model of LTx

a) Representative immunohistochemistry staining of M1-macrophages, stained for NOS2, (scale bar of 50µm); b) relative quantification via CAST system of NOS2+ cells in the left lung graft of LTx mice, 2 months after LTx; c) Representative immunohistochemistry staining of M2-macrophages stained for CD206 (scale bar of 50µm) and d) relative quantification via CAST

system of CD206+ cells in the left lung graft of LTx mice, 2 months after LTx. Violin plots represent mean values. Statistical significance was assessed using Mann-Whitney U test.

References

1. Kneidinger N, Milger K, Janitza S, et al. Lung volumes predict survival in patients with chronic lung allograft dysfunction. *Eur Respir J* 2017; 49.
2. Meyer KC, Raghu G, Verleden GM, et al. An international ISHLT/ATS/ERS clinical practice guideline: diagnosis and management of bronchiolitis obliterans syndrome. *Eur Respir J* 2014; 44: 1479-1503.
3. Verleden GM, Glanville AR, Lease ED, et al. Chronic lung allograft dysfunction: Definition, diagnostic criteria, and approaches to treatment-A consensus report from the Pulmonary Council of the ISHLT. *J Heart Lung Transplant* 2019; 38: 493-503.
4. Meyer KC, Raghu G, Baughman RP, et al. An official American Thoracic Society clinical practice guideline: the clinical utility of bronchoalveolar lavage cellular analysis in interstitial lung disease. *Am J Respir Crit Care Med* 2012; 185: 1004-1014.
5. Smirnova NF, Conlon TM, Morrone C, et al. Inhibition of B cell-dependent lymphoid follicle formation prevents lymphocytic bronchiolitis after lung transplantation. *JCI insight* 2019; 4.
6. Stewart S, Fishbein MC, Snell GI, et al. Revision of the 1996 working formulation for the standardization of nomenclature in the diagnosis of lung rejection. *J Heart Lung Transplant* 2007; 26: 1229-1242.
7. Verleden SE, Vos R, Vanaudenaerde BM, et al. Chronic lung allograft dysfunction phenotypes and treatment. *J Thorac Dis* 2017; 9: 2650-2659.
8. Glanville AR, Aboyoun CL, Havryk A, et al. Severity of lymphocytic bronchiolitis predicts long-term outcome after lung transplantation. *Am J Respir Crit Care Med* 2008; 177: 1033-1040.
9. Boehler A, Chamberlain D, Kesten S, et al. Lymphocytic airway infiltration as a precursor to fibrous obliteration in a rat model of bronchiolitis obliterans. *Transplantation* 1997; 64: 311-317.
10. Chen X, Cho DB, Yang PC. Double staining immunohistochemistry. *N Am J Med Sci* 2010; 2: 241-245.
11. Adams TS, Schupp JC, Poli S, et al. Single-cell RNA-seq reveals ectopic and aberrant lung-resident cell populations in idiopathic pulmonary fibrosis. *Sci Adv* 2020; 6.
12. Morse C, Tabib T, Sembrat J, et al. Proliferating SPP1/MERTK-expressing macrophages in idiopathic pulmonary fibrosis. *Eur Respir J* 2019; 54.
13. Habermann AC, Gutierrez AJ, Bui LT, et al. Single-cell RNA sequencing reveals profibrotic roles of distinct epithelial and mesenchymal lineages in pulmonary fibrosis. *Sci Adv* 2020; 6: eaba1972.

Fig. Supplementary 1

a

	Stable	BOS
Number of patients	20	22
Age (years)	43 ±8	47 ±12
Sex	13 female, 7 male	8 female, 14 male
Underlying disease	COPD 2	COPD 1
	LF 8	LF 11
	CF 6	CF 4
	PH 4	PH 6
Procedure (SLTx, DLTx)	All DLTX	All DLTX
Days BAL after LTx	513	759
Grade at BAL	All 0	BOS-0 n=20 (90.9%)
		BOS-1 n=13 (59%)
		BOS-2 n=13 (59%)
		BOS-3 n=20 (90.9%)
BAL cell count	5,8	9,6
Blood LDH	258	261
Home spirometry devise daily	all	all

Stable (n=20)

55% had bronchoscopy within 12 months

15% had suspicious of allograft dysfunction without a sign of infection or rejection on bronchoscopy and sign of dysfunction were only transient

10% had bronchoscopy to out infection with no sign of infection in BAL

10% had bronchoscopy anastomotic stenosis (one only for suspicion and one dilatation of moderate anastomotic stenosis

5% patient no obvious reason was found

5% patient surveillance after switch of immunosuppression

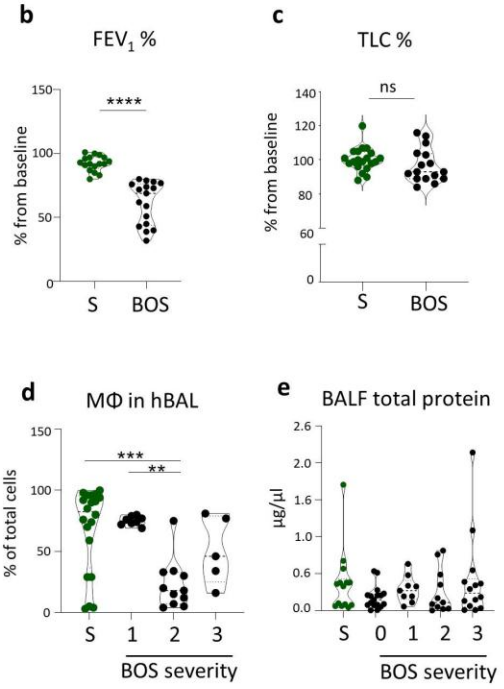

f

Underlying disease	LTx type	Age, Sex	Rejection grade	Therapy	Complications	Time before reTx
PAH	Heart-lung	31, F	Stage-3 BOS	Immunosuppressive drugs	Aspergillus aereus	nd
PAH and histiocitosis	SLTx	42,F			Edema, Staphylococcus aureus, CMV infection	nd
IPD	DLTx	41, F			Aspergillus aureus, Fibrotic pneumopathy	7 years
nd	Heart-lung	F				6 years
PAH		41,F			infection	2 years

Fig. Supplementary 2

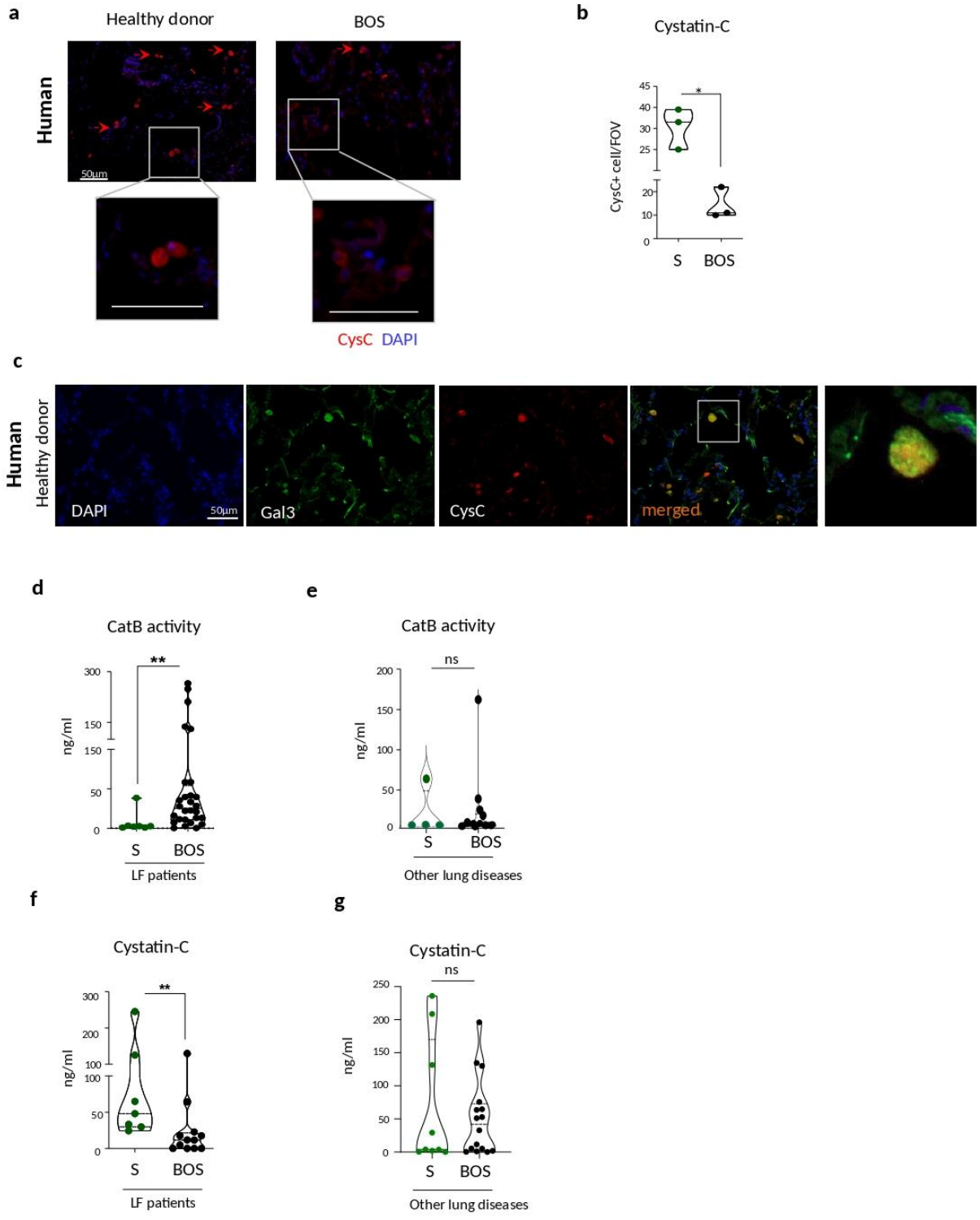

Fig. Supplementary 3

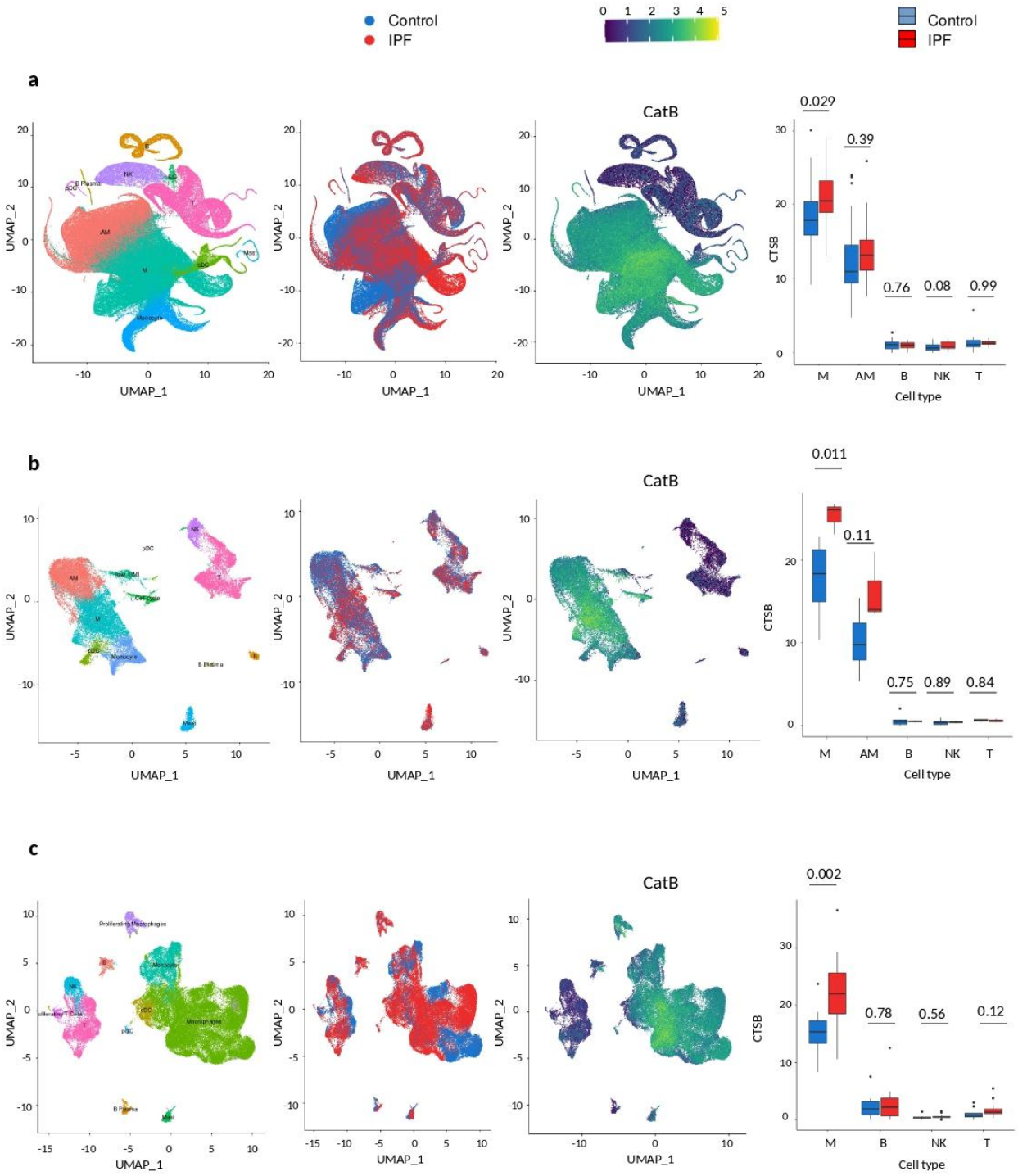

Fig. Supplementary 4

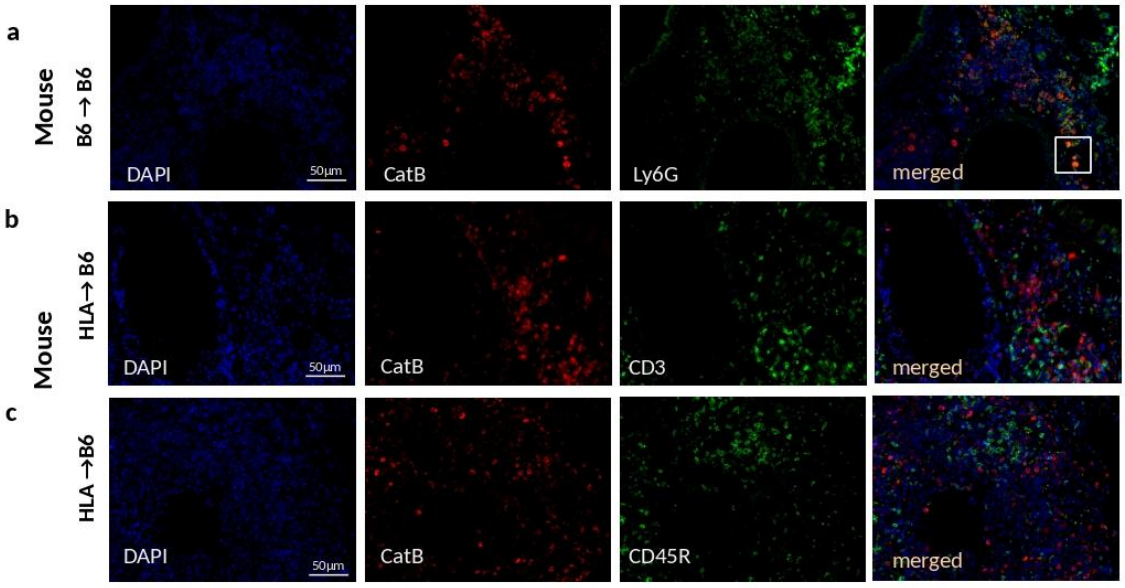
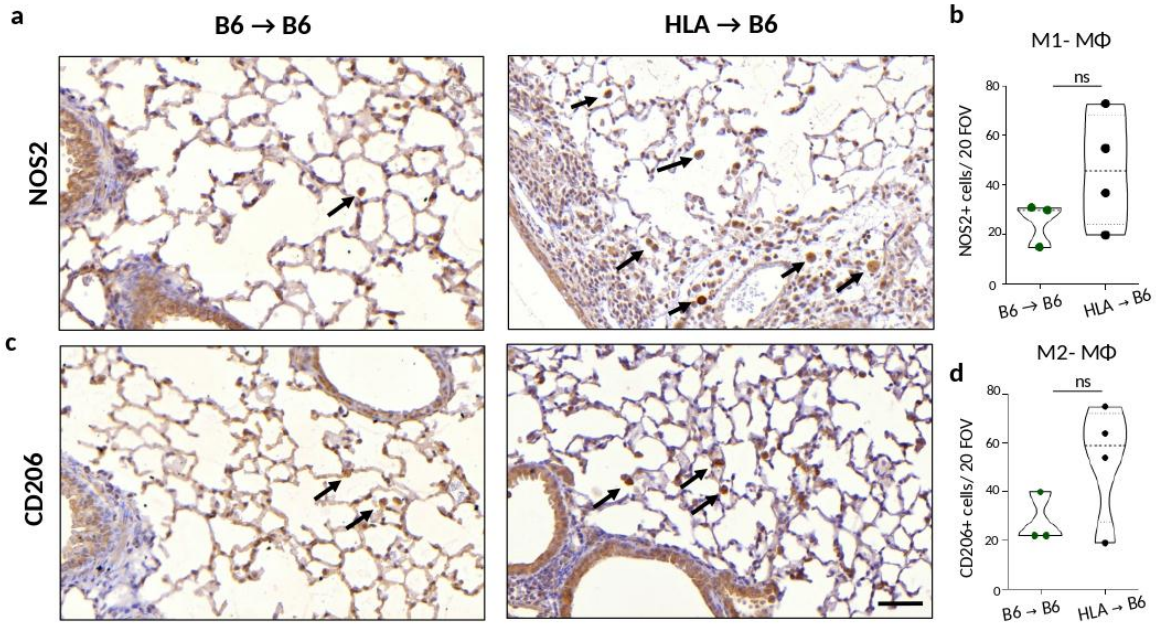
Fig. Supplementary 5